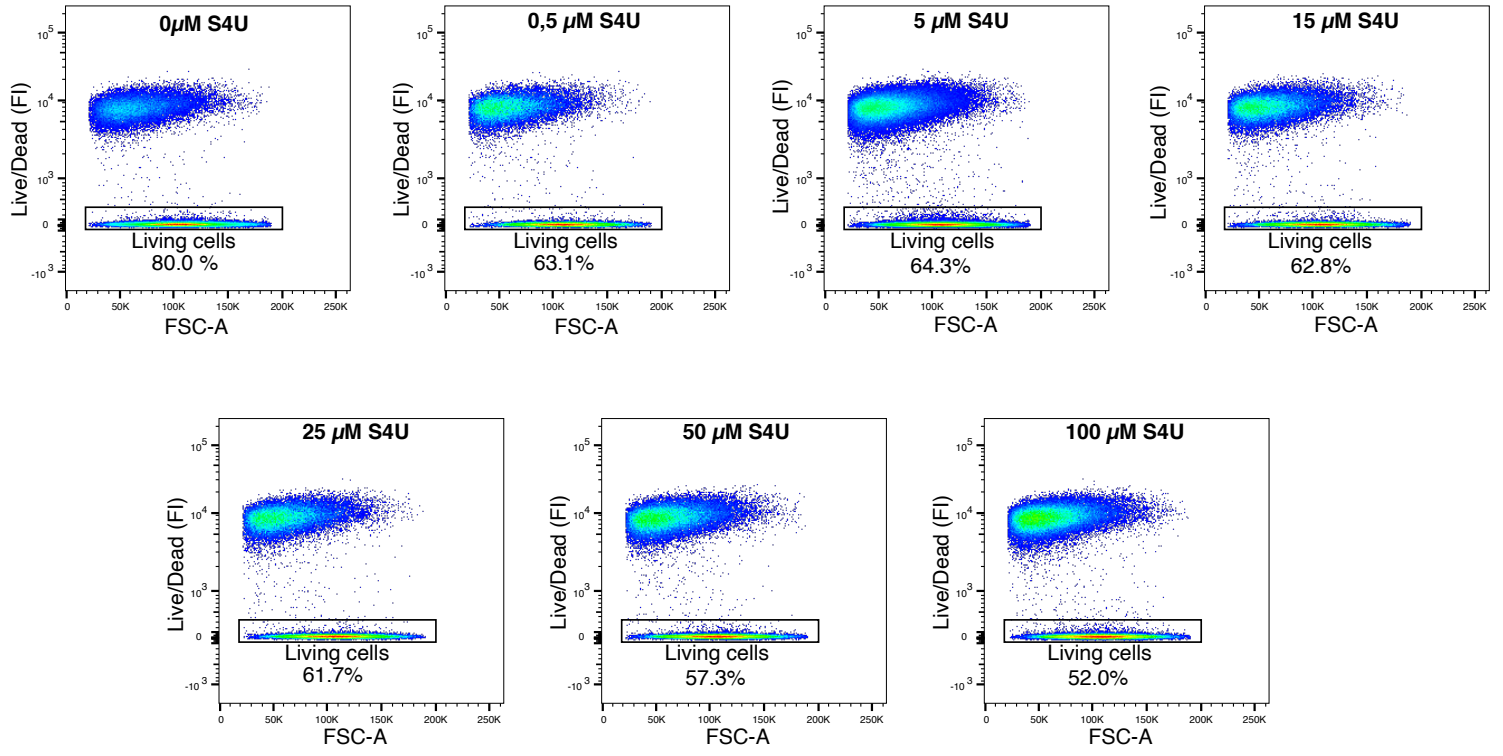


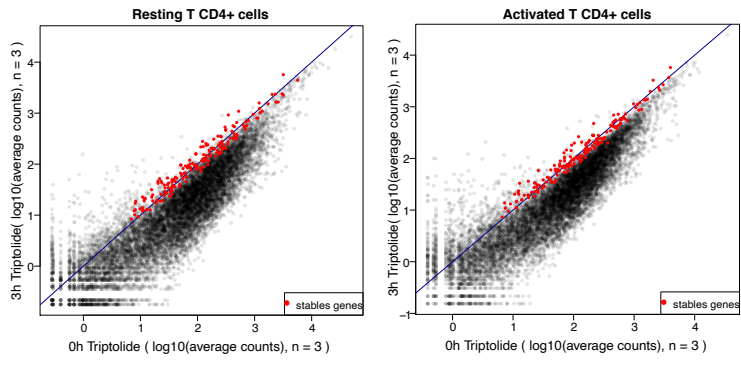
Supplemental Figure 1



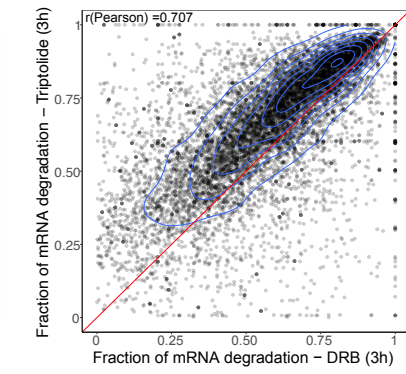
Supplemental Figure 1. Cell viability of primary CD4+ T cells incubated with different concentrations of 4-Thiouridine. Primary CD4+ T cells were incubated in the presence of different concentrations of 4-Thiouridine for 24h (the medium was replaced every three hours with fresh medium containing 4-Thiouridine). Cell viability is measured by flow cytometry using Live/Dead ef780 labeling.

Supplemental Figure 2

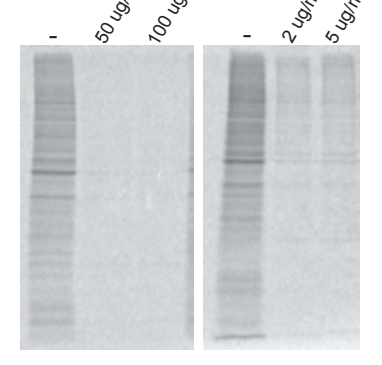
A.



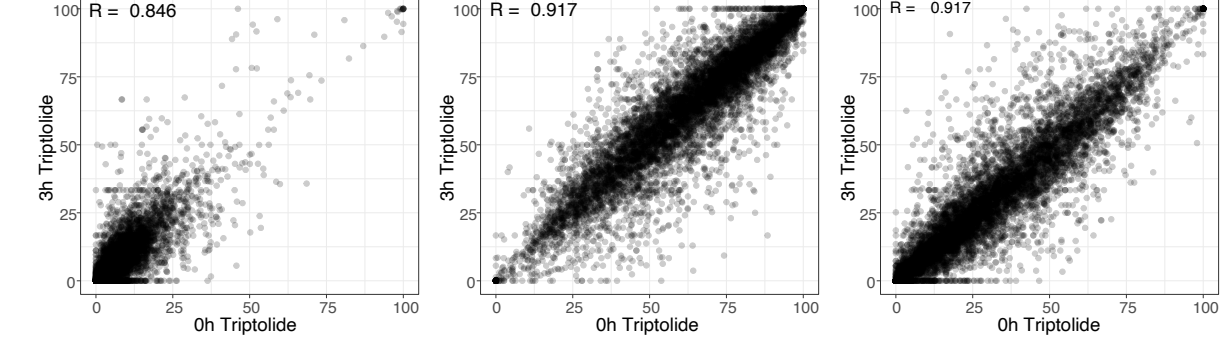
B.



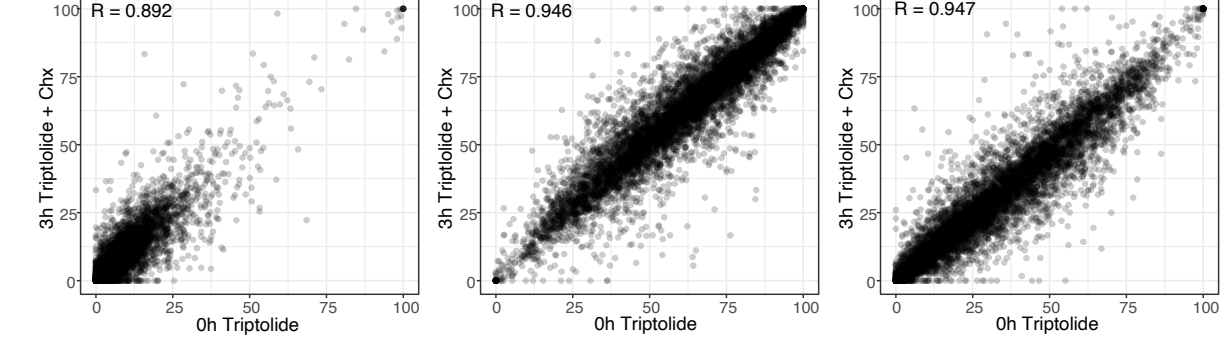
C.



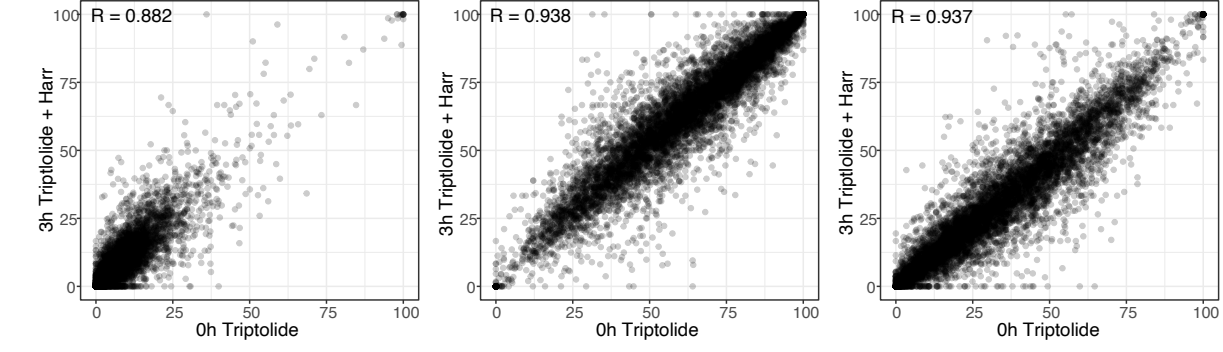
D.



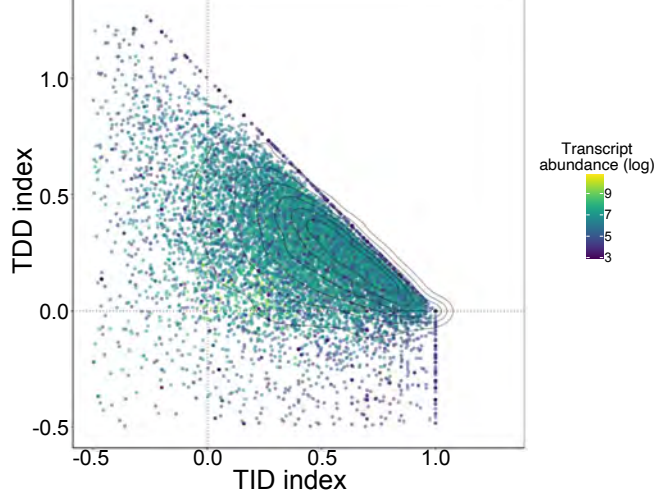
E.



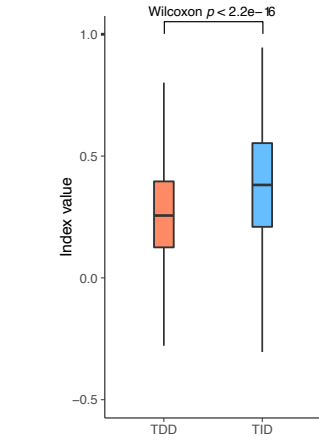
F.



G.



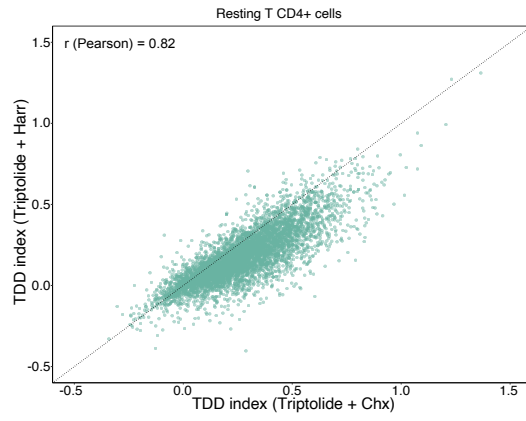
H.



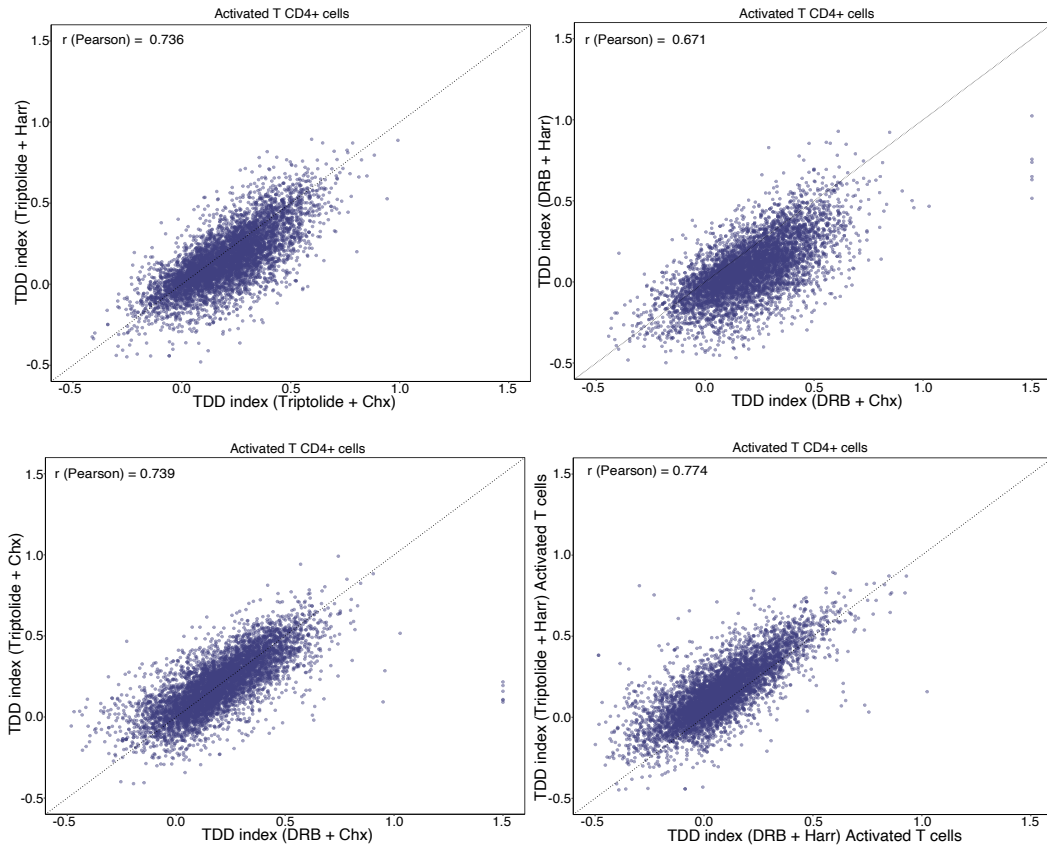
Supplemental Figure 2. Normalization of RNA-seq datasets with stable transcripts, reads distribution upon transcription and translation inhibition and Gene Ontology analyses. **A.** Scatter-plots of RNA-seq read counts in control cells against read counts in cells incubated for 3 hours in the presence of triptolide. Red dots correspond to the stable transcripts that were selected to normalize gene expression upon transcription inhibition. **B.** Scatter plot of the fraction of observed mRNA degradation in T CD4+ cells incubated with Triptolide or DRB for 3h. **C.** Metabolic labeling of resting CD4+ T cells using S³⁵ methionine in the absence and presence of different doses of cycloheximide and harringtonine. **D to F.** Scatter-plots comparing, for each transcript, the percentage of reads mapping to the 5'UTR, CDS and 3'UTR in the control and triptolide 3h (**D**) or in the control and triptolide + cycloheximide 3h (**E**) or in the control and triptolide + harringtonine (**F**) RNA-seq libraries. **G.** Scatter plot of TDD indexes against TID indexes from resting CD4+ T cells. **H.** Box plot of the distribution of TDD and TID indexes in resting cells and statistical assessment of the difference using a Wilcoxon-rank test.

Supplemental Figure 3

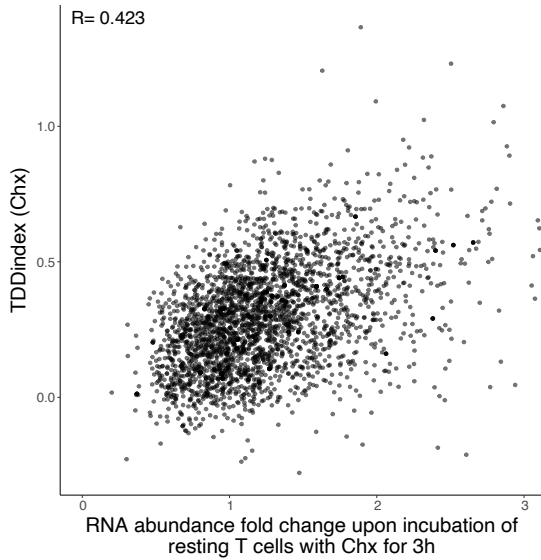
A.



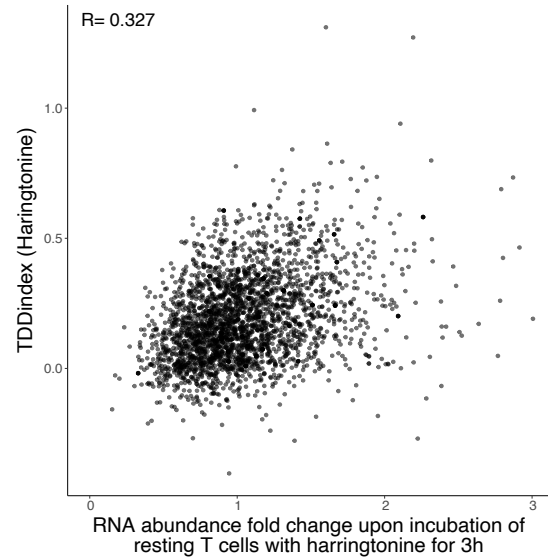
B.



C.



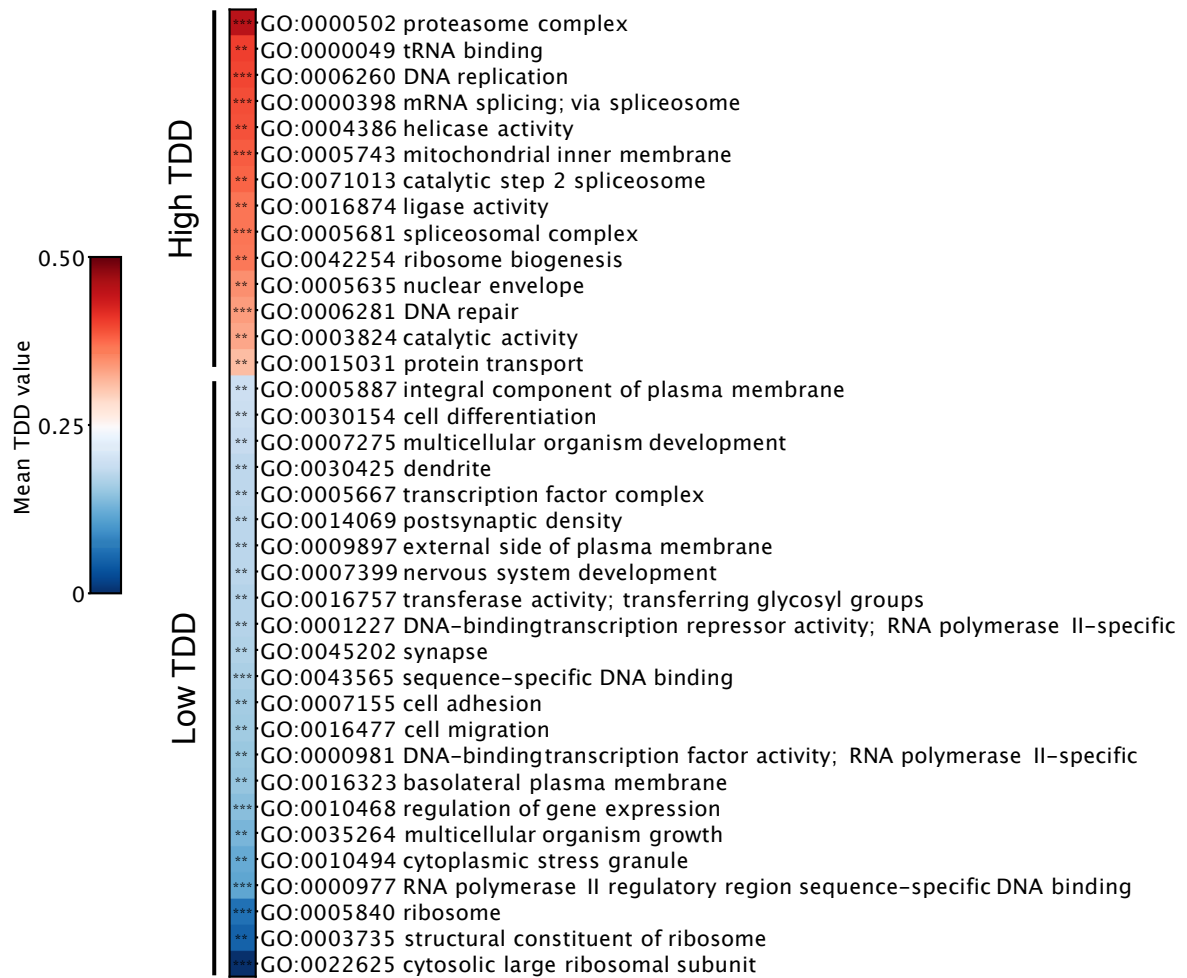
D.



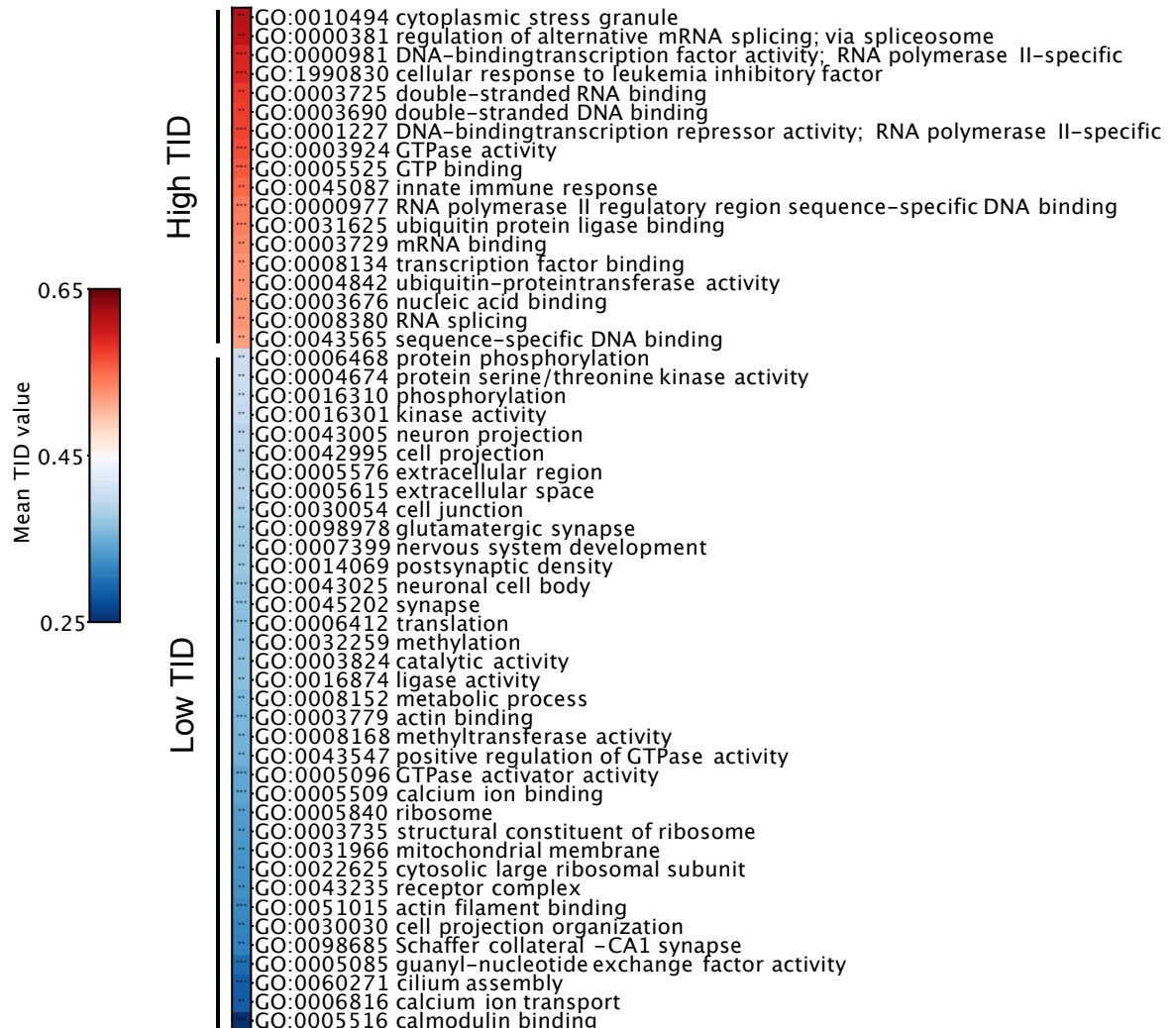
Supplemental Figure 3. A. Scatter-plot comparing the TDDindexes obtained from resting T cells incubated with cycloheximide or harringtonine. **B.** Scatter-plots of the TDDindexes calculated using different combinations of transcription and translation inhibitors in activated T cells. **C.** Scatter-plot comparing the TDDindex obtained using triptolide and cycloheximide against the fold-change in transcript abundance obtained from cells incubated in the presence of cycloheximide or not and in the absence of any transcription inhibitor. **D.** Same as **C** but in cells incubated the presence of harringtonine as a translation inhibitor.

Supplemental Figure 4

A.



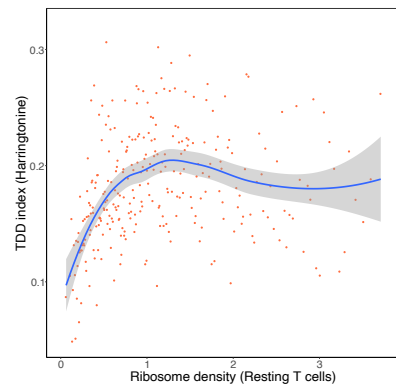
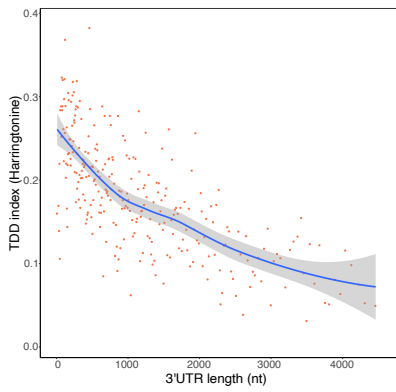
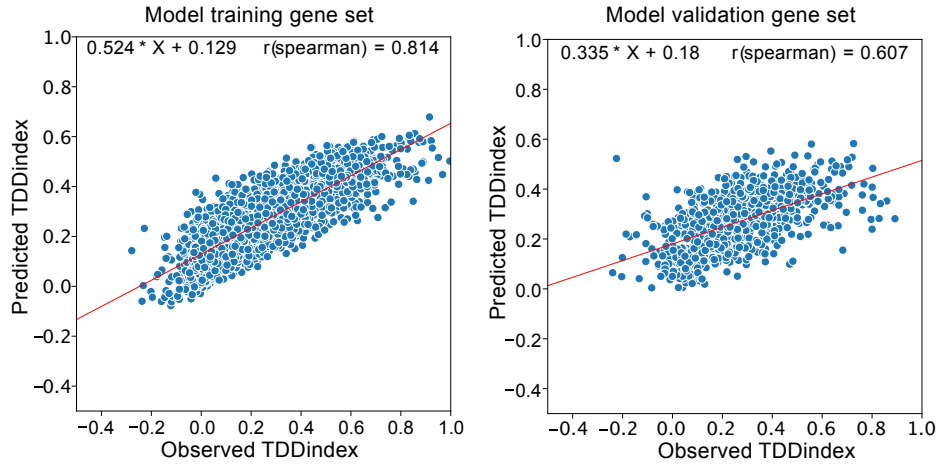
B.



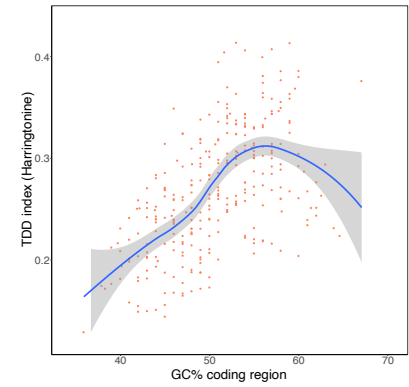
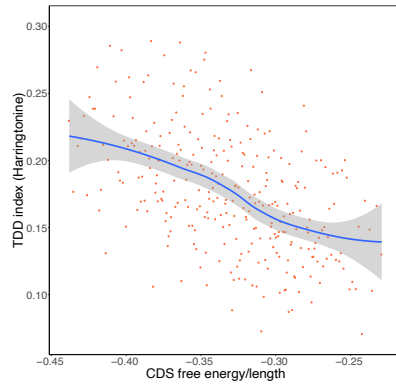
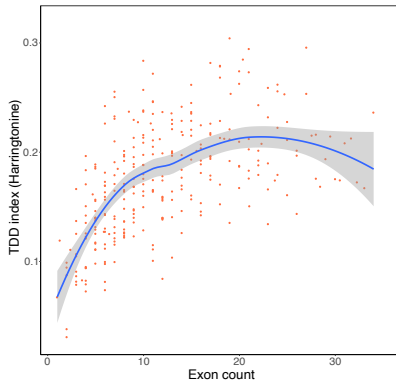
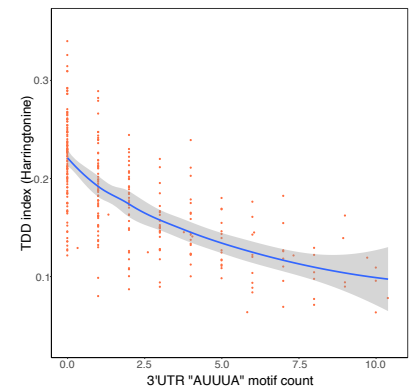
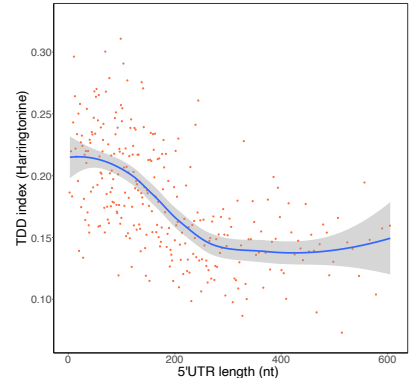
Supplemental Figure 4. A. List of Gene Ontology terms with a median TDDindex that is significantly higher (red) or lower (blue) from the median TDDindex of the entire transcript population. **B.** Same analysis as (A.) but using the TIDindex.

Supplemental Figure 5

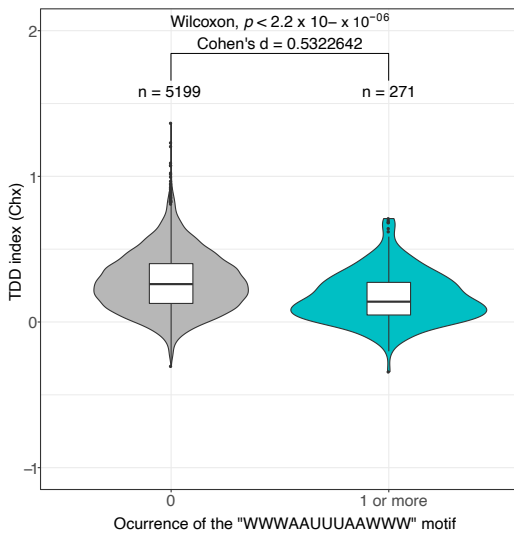
A.



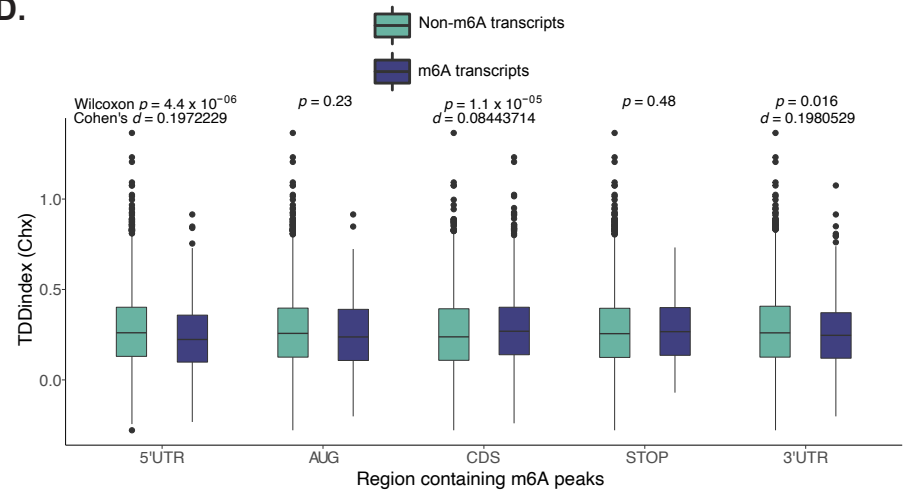
B. Resting T CD4+ cells (Harringtonine)



C.



D.



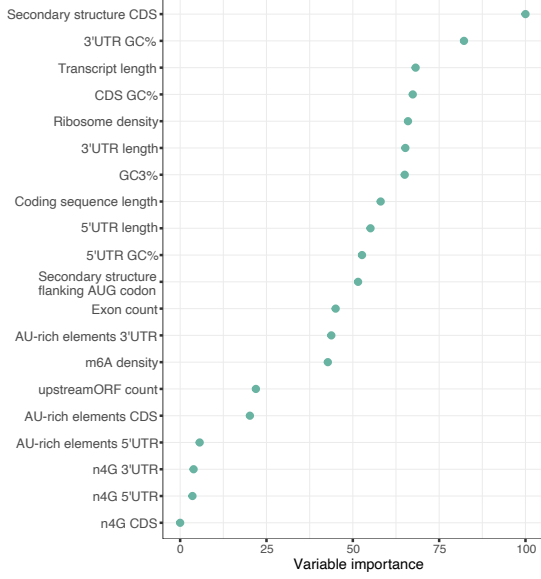
Supplemental Figure 5. A. Scatter plots of predicted versus observed TDD index values from the training gene set used to generate the random forest model (left panel) and the validation gene set that was not use to generate the model. **B.** Binning plots of TDDindex obtained using harringtonine, instead of cycloheximide, against different transcript features. **C.** Violin-plot of TDDindex obtained with cycloheximide for transcripts with no “WWWAAUUUAAWWW” motif or 1 or more motifs in their 3’UTR and statistical assessment of the difference using a Wilcoxon-rank test. Displayed p-value corresponds to the mean p-value of a Wilcoxon test performed 1000 independent times on samples of the same size for each compared group. The Cohen’s d value is also displayed to evaluate the effect size.

D. Box-plot of the TDDindex in transcripts bearing m6A sites (m6A transcripts) or not (Non-m6A transcripts) among different transcripts regions and statistical assessment of the difference using a Wilcoxon-rank test. The Cohen’s d value is also displayed to evaluate the effect size.

Supplemental Figure 6

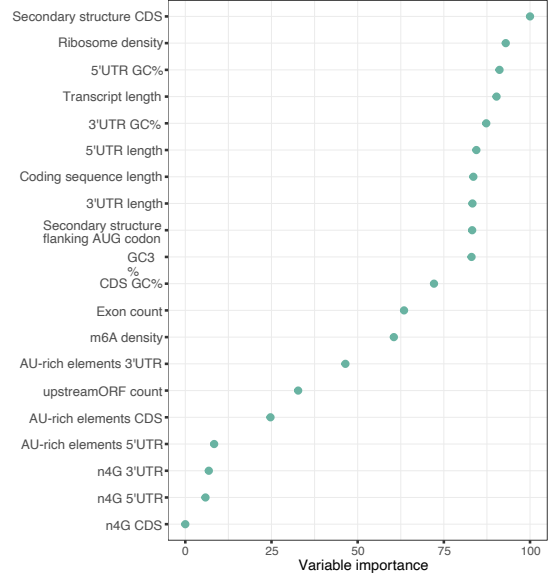
A.

Random forests model to explain the fold-change in RNA abundance obtained upon incubation of cells with cycloheximide

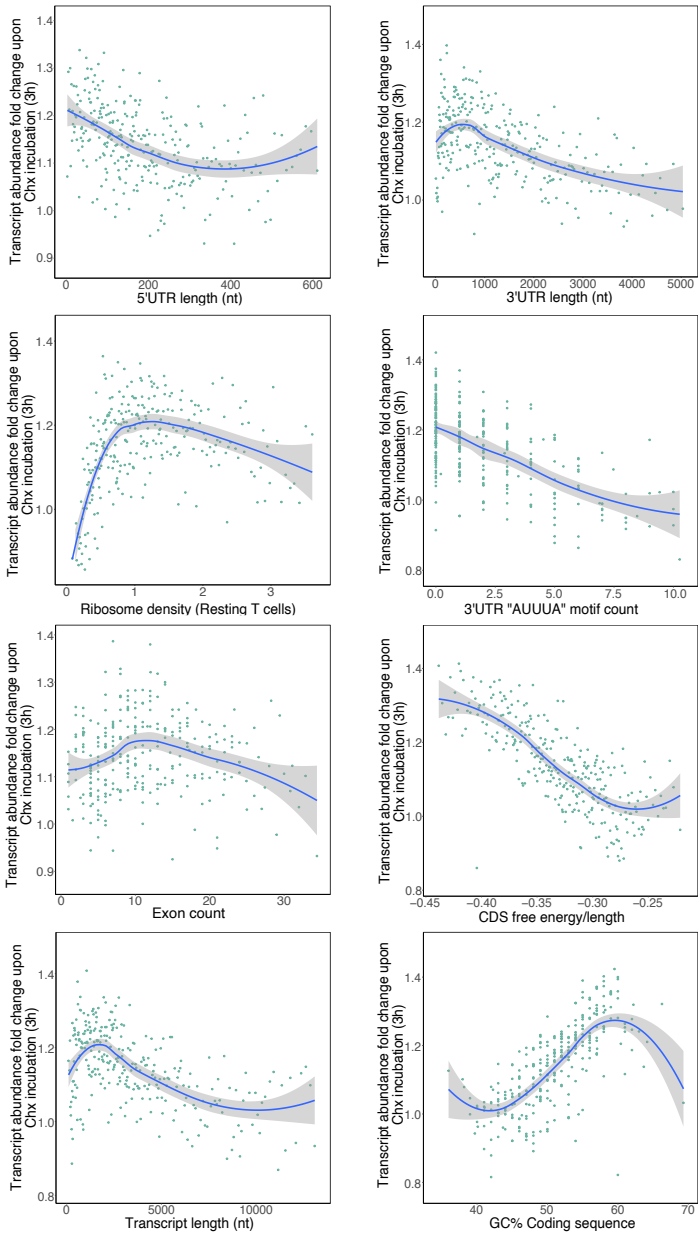


B.

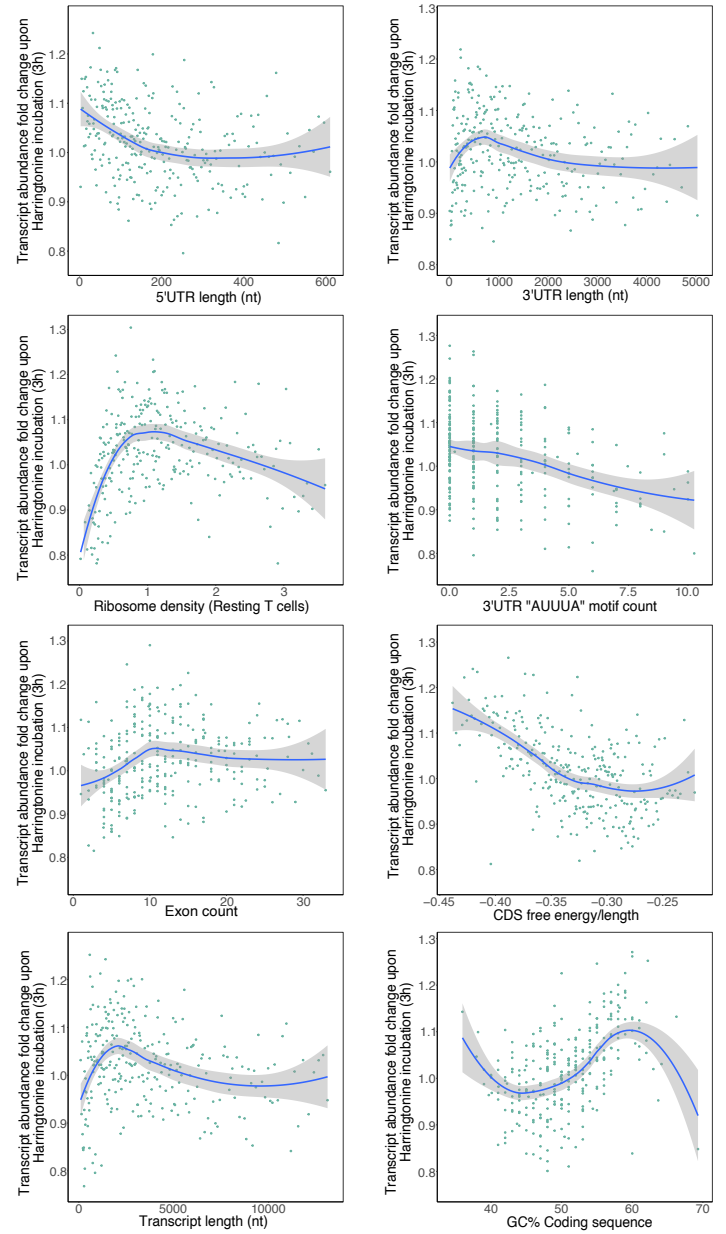
Random forests model to explain the fold-change in RNA abundance obtained upon incubation of cells with harringtonine



C.

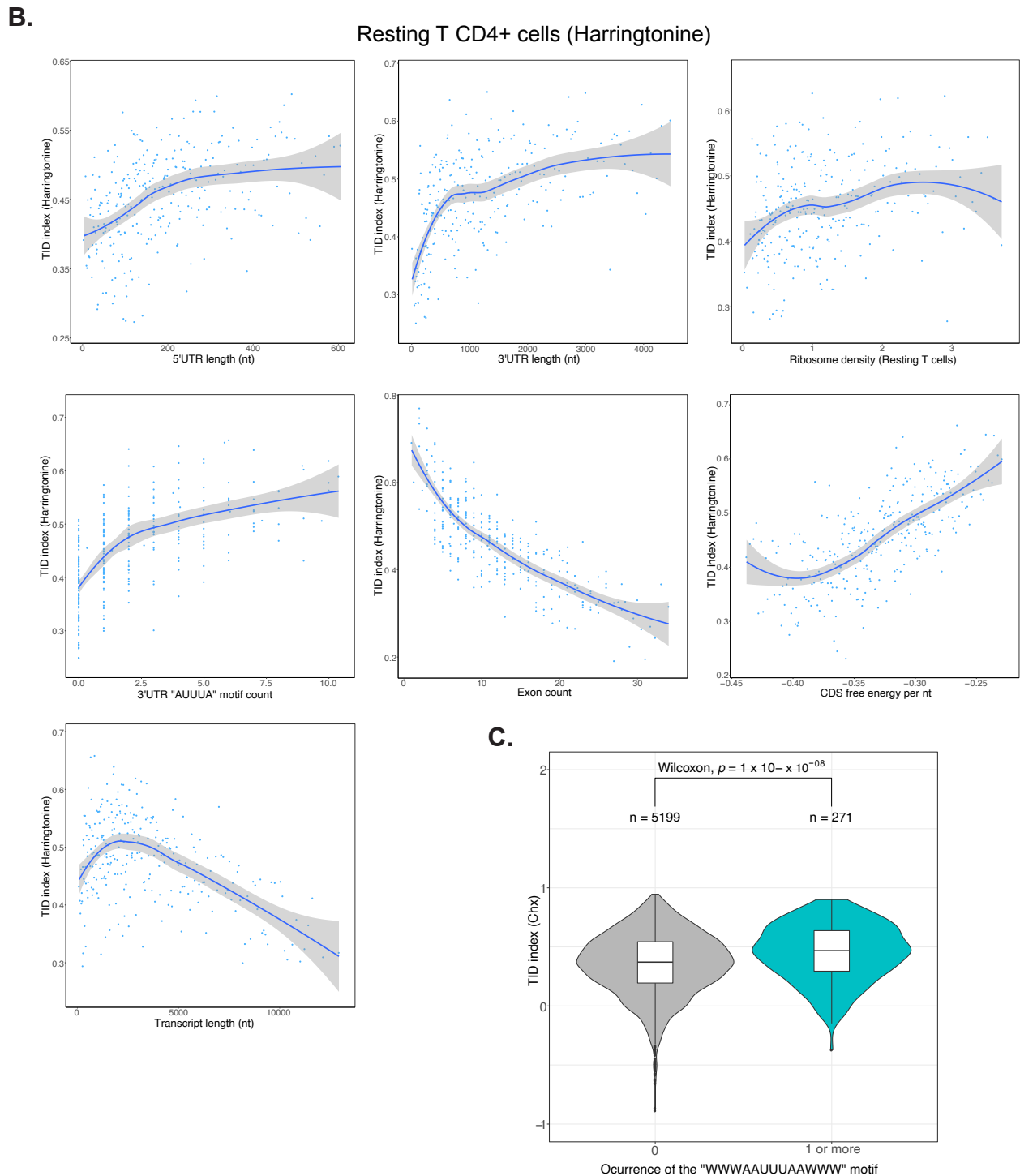
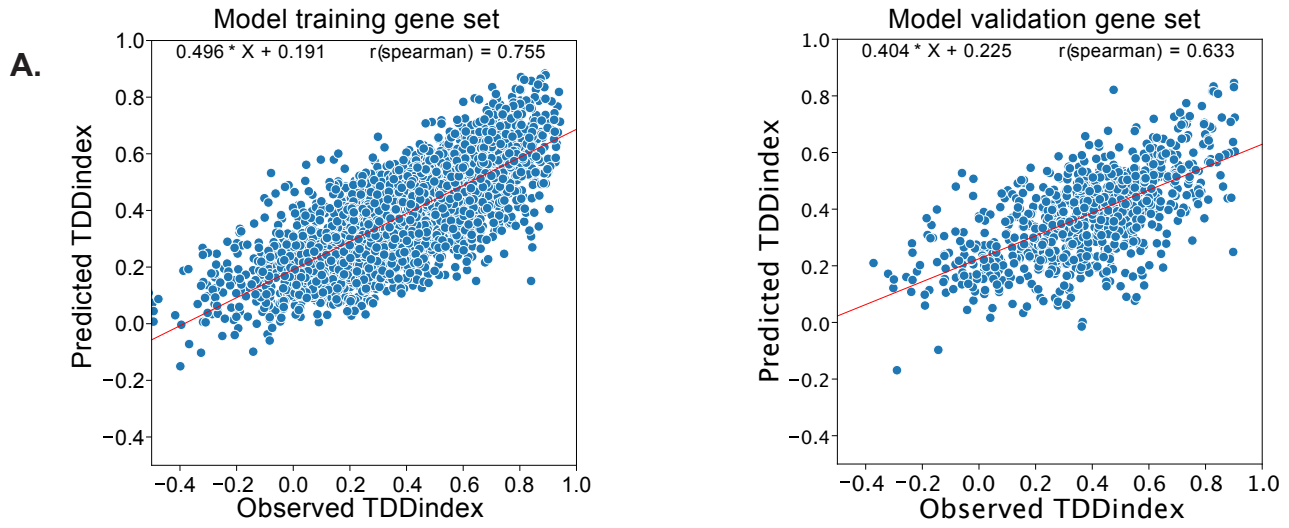


D.



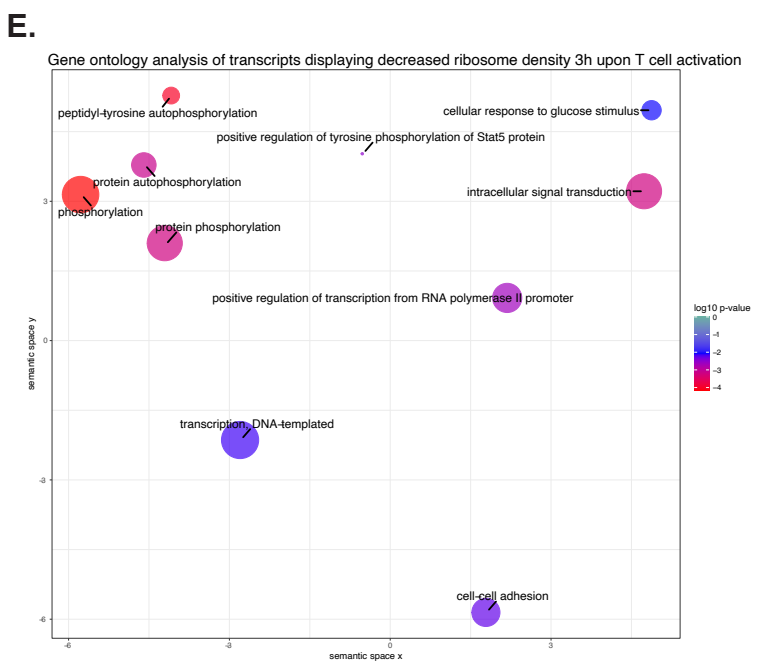
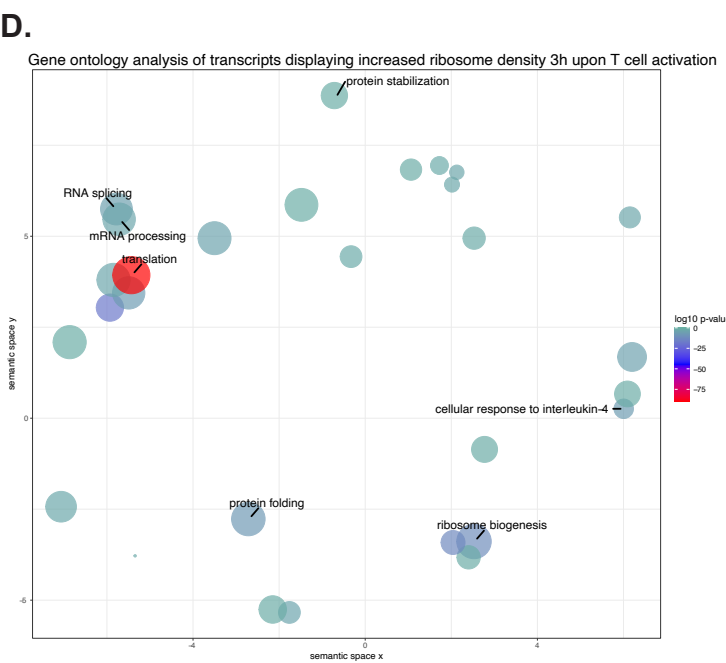
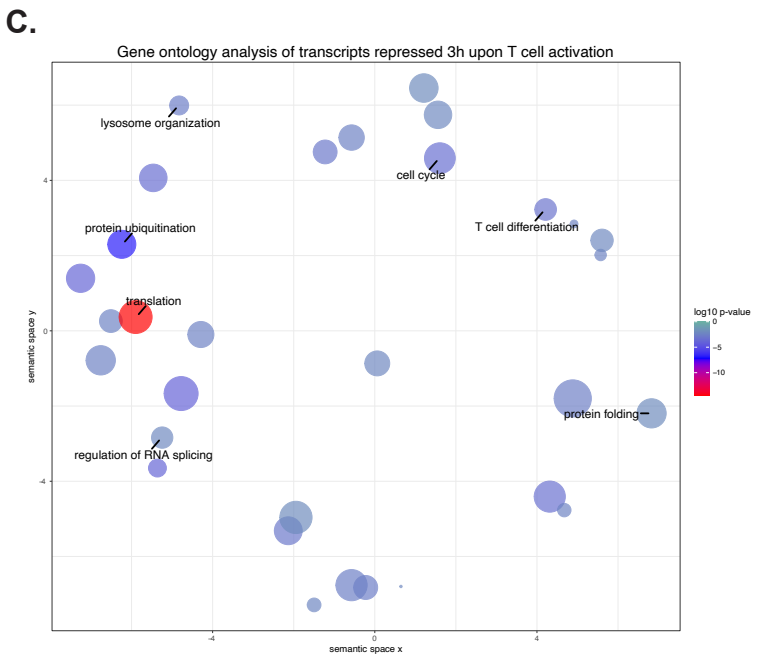
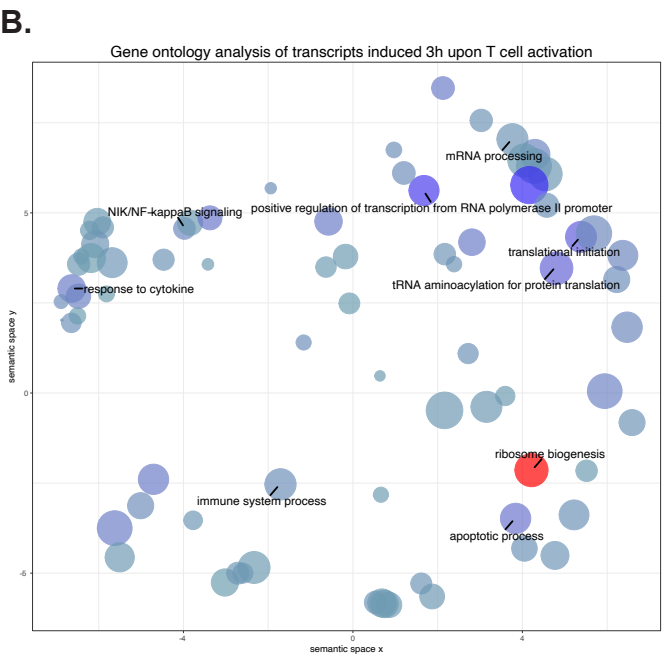
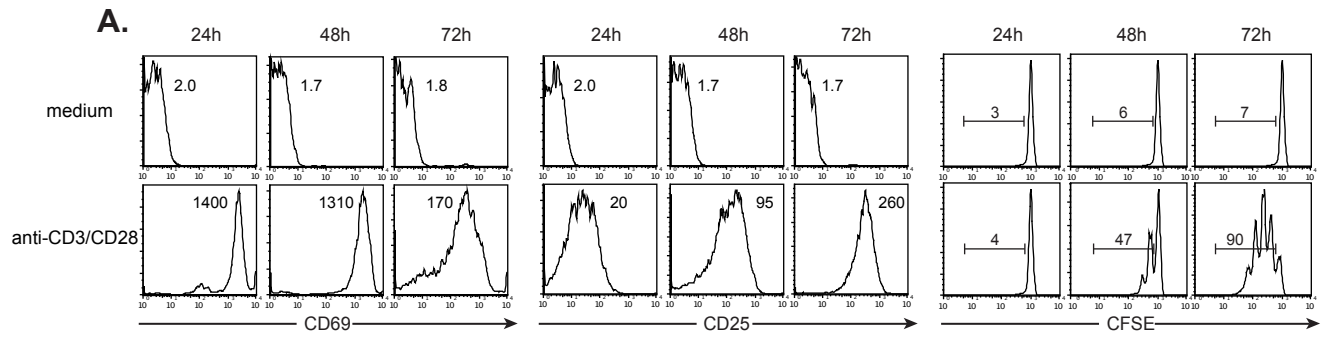
Supplemental Figure 6. A. Random forest decision trees analysis of transcript features to explain the observed fold-change in transcript abundance obtained when comparing resting CD4+ T cells incubated in the presence of cycloheximide or not. Features are sorted from top to bottom with respect to their importance in predicting the TDDindex. **B.** Binning plots of the fold-change in transcript abundance when cells are incubated in the presence of cycloheximide or not, against different transcript features. **C** and **D.** Same as **A** and **B** but in cells incubated with harringtonine instead of cycloheximide.

Supplemental Figure 7



Supplemental Figure 7. A. Scatter plots of predicted versus observed TID index values from the training gene set used to generate the random forest model (left panel) and the validation gene set that was not use to generate the model. **B.** Binning plots of TIDindex obtained using harringtonine, instead of cycloheximide, against different transcript features. **C.** Violin-plot of TIDindex obtained with cycloheximide for transcripts with no “WWWAAUUUAAWWW” motif or 1 or more motifs in their 3’UTR.

Supplemental Figure 8

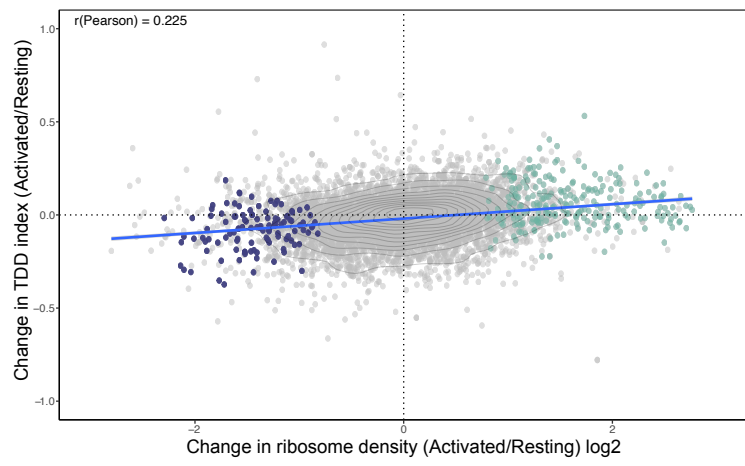


Supplemental Figure 8. Gene Ontology analysis of differentially expressed and translated transcripts upon CD4+ T cell activation. **A.** Flow cytometry analysis of the cell activation markers (CD69 and CD25) as well as cell division (CFSE staining) in resting CD4+ T lymphocytes (top panels) or upon activation for 24, 48 and 72 hours in presence of anti-CD3/CD28 magnetic beads. **B-E.** Analysis of enriched functional gene categories among (**B.**) Transcripts whose expression is up-regulated upon T cell activation; (**C.**) Transcripts whose expression is down-regulated upon T cell activation; (**D.**) Transcripts whose ribosome density increases upon T cell activation; (**E.**) Transcripts whose ribosome density decreases upon T cell activation. Analysis were performed using REVIGO (Supek et al. 2011). Each circle corresponds to a given Gene Ontology category, the radius being linked to its size (in gene number) and the color corresponding to the adjusted p-value of the observed enrichment. The x and y axes correspond to arbitrary positions defined by REVIGO to facilitate separation and reading of enriched GO terms.

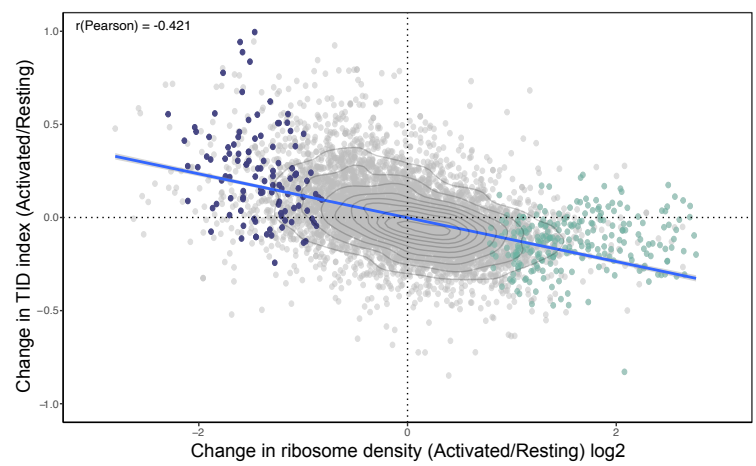
Supplemental Figure 9. Relationship between GC content in the coding sequence, TDD and TID. **A.** Relative abundance of GC3 and AU3 codons among codons with positive and negative CSCs in resting (left panel) and activated (right panel) CD4+ T cells. **B.** Comparison of observed codon stability coefficient for the TDDindex in resting (green bars) and activated (violet bars) T CD4+ lymphocytes. **C.** Same as (A.) but using TIDindex instead of TDDindex. **D.** Same as (B.) but using TIDindex instead of TDDindex.

Supplemental Figure 10

A.

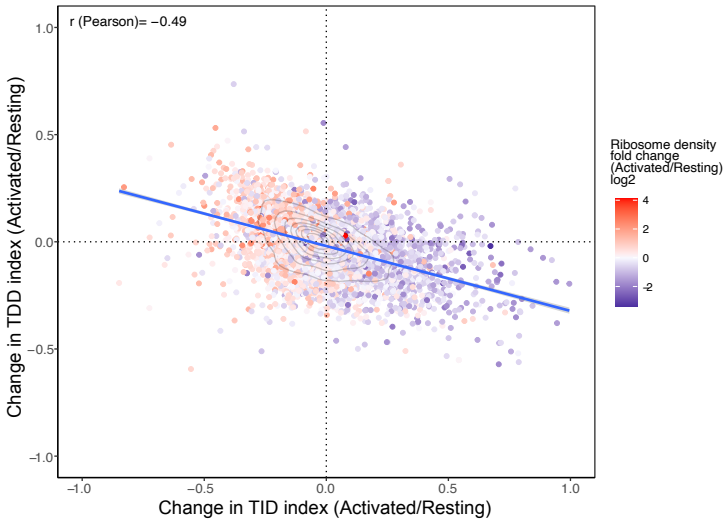


B.

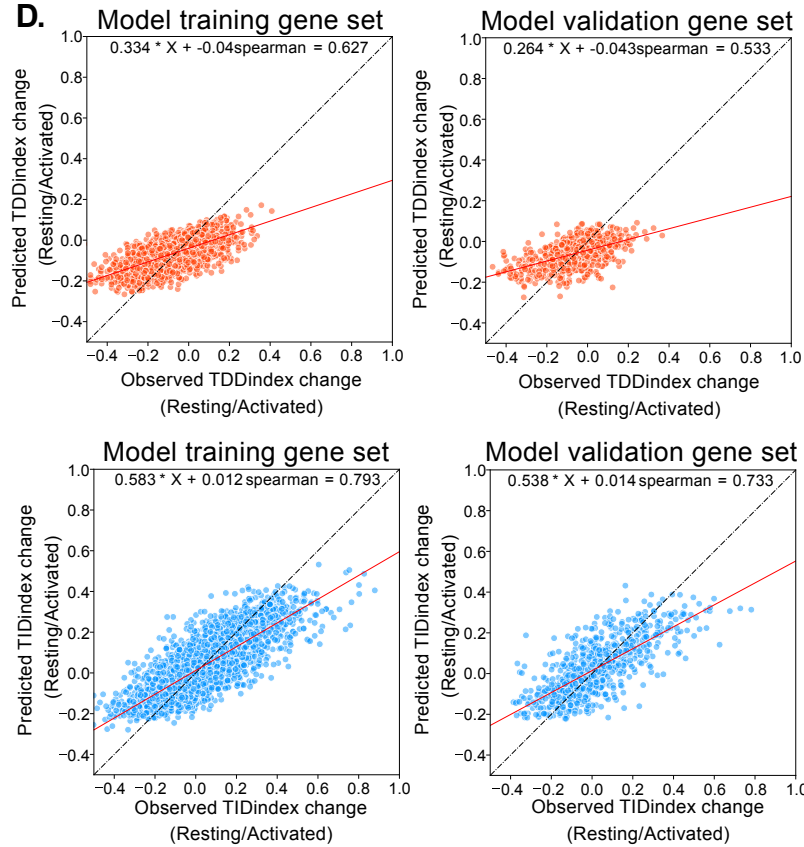


C.

Delta TDDindex Vs Delta TIDindex (Activated/Resting) Harringtonine

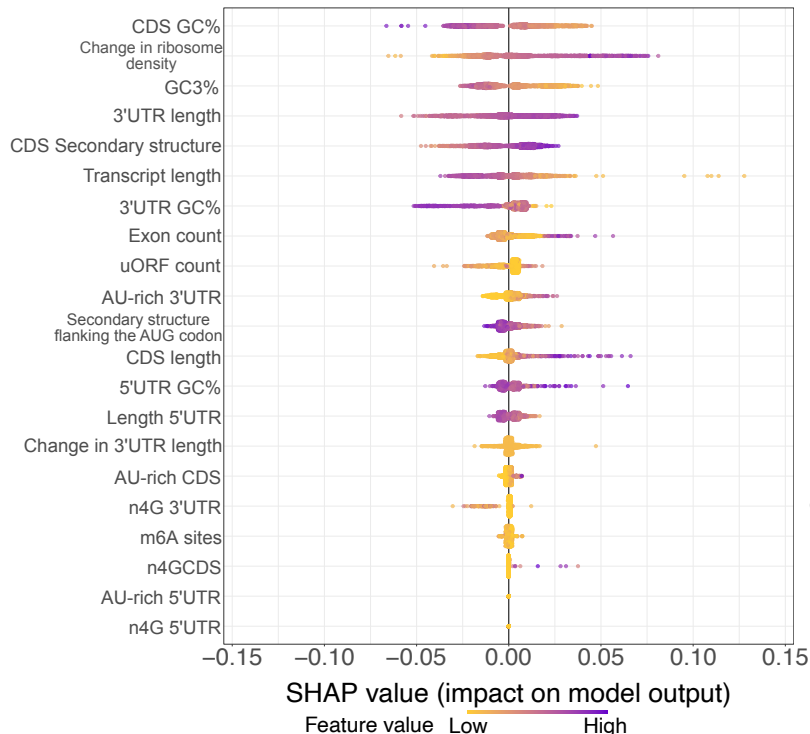


D.

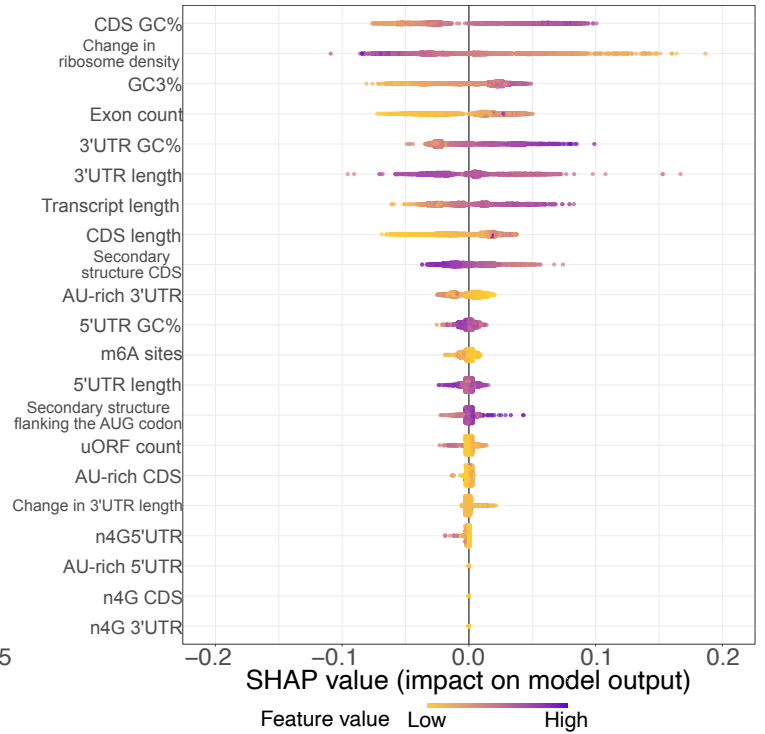


E.

Random forest analysis of the observed change in TDD index between resting and activated T CD4+ cells



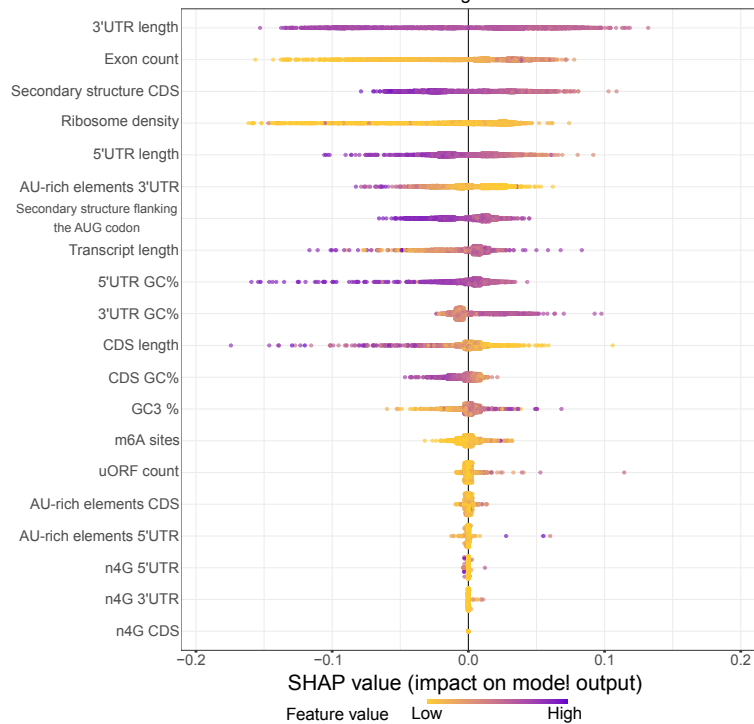
Random forest analysis of the observed change in TID index between resting and activated T CD4+ cells



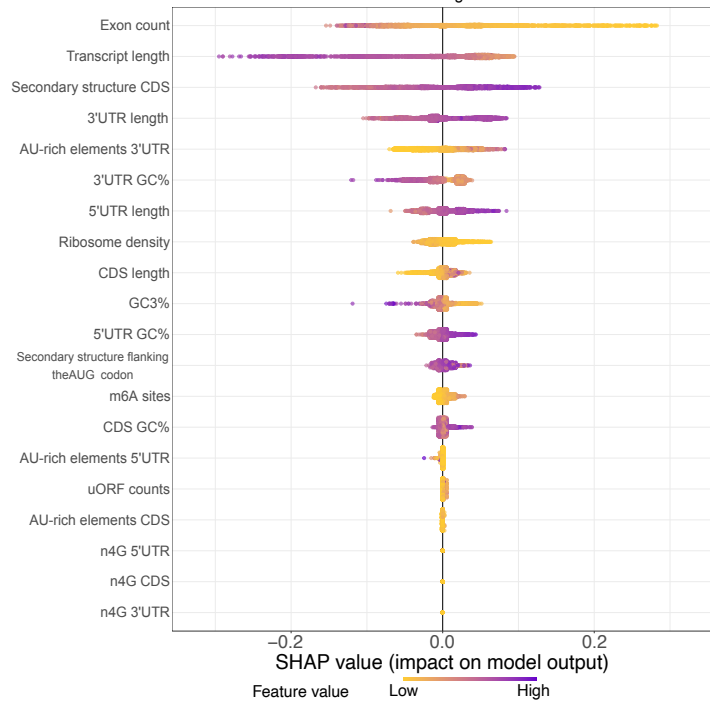
Supplemental Figure 10. Changes in ribosome density upon T cell activation modulate both TDD and TID. **A.** Scatter plot of the changes in ribosome density between resting and activated cells (x axis) against the changes in the TDD index (y axis) obtained using harringtonine instead of cycloheximide. Each dot corresponds to a single transcript **B.** Scatter plot of the changes in ribosome density between resting and activated cells (x axis) against the changes in the TID index (y axis) obtained using harringtonine instead of cycloheximide. **C.** Scatter plot of the change in TDDindex (y axis) and TIDindex (x axis) between resting and activated cells obtained using harringtonine. Transcripts are colored with respect to the change in ribosome density measured between resting and activated cells. **D.** Scatter plots of predicted versus observed changes in TDD index (top panels) and changes in TID index (bottom panels), upon T cell activation, from the training gene set used to generate the random forest model (left panels) and the validation gene set that was not use to generate the model (right panels). **E.** Random forest analysis of the changes in TDDindex (left panel) and TIDindex (right panel) between resting and activated CD4+ T cells.

Supplemental Figure 11

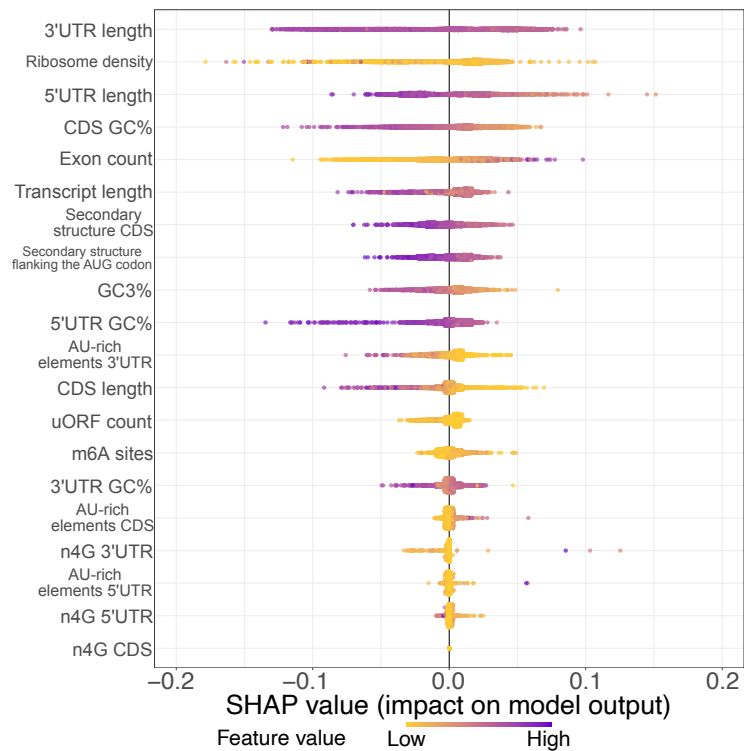
Random forests model to explain TDDindex distribution in Resting CD4+ T Cells



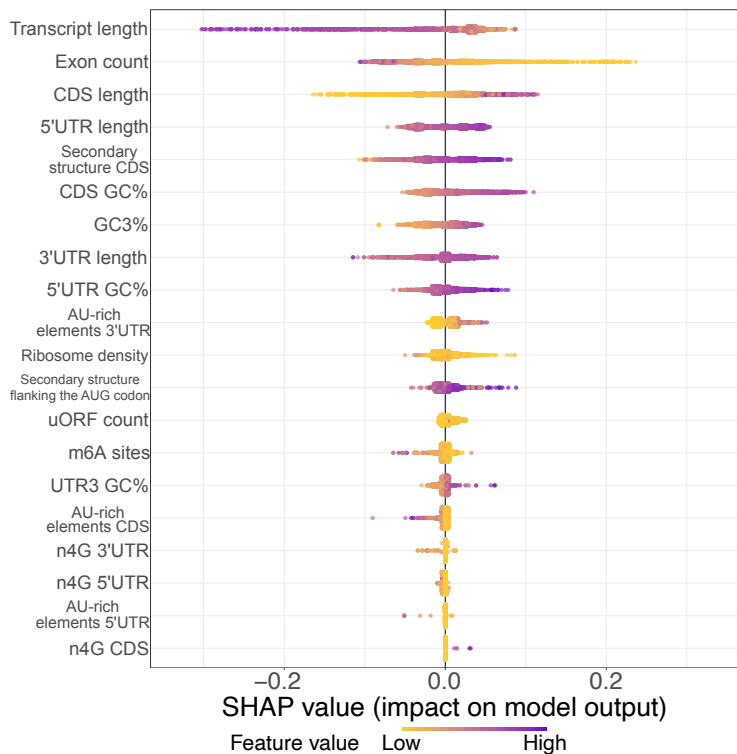
Random forests model to explain TIDindex distribution in Resting CD4+ T Cells



Random forests model to explain TDDindex distribution in Activated CD4+ T Cells



Random forests model to explain TIDindex distribution in Activated CD4+ T Cells



Supplemental Figure 11. SHAP value plots for all random forest analyses in resting and activated cells.